Engineering Notes

ENGINEERING NOTES are short manuscripts describing new developments or important results of a preliminary nature. These Notes cannot exceed 6 manuscript pages and 3 figures; a page of text may be substituted for a figure and vice versa. After informal review by the editors, they may be published within a few months of the date of receipt. Style requirements are the same as for regular contributions (see inside back cover).

An Unsteady Wake Model for a Hingeless Rotor

S. T. Crews,* K. H. Hohenemser†
Washington University, St. Louis, Mo.
and
R. A. Ormiston‡
U.S. Army Air Mobility R&D Laboratory, Moffett Field, Calif.

Nomenclature

A = aerodynamic blade constant
B = tiploss factor
L = inflow gain
R = rotor radius
t = nondimensional time with unit $1/\Omega$
β = blade flapping angle, positive up
γ = blade lock number
λ = inflow angle, constant over radius
θ = blade pitch angle, positive nose-up
Ω = rotor angular speed
ω = nondimensional frequency in rotating frame with unit Ω
ω_f = nondimensional frequency in fixed frame
ω_1 = nondimensional blade natural frequency
τ = inflow time constant
ϕ = phase angle difference between β and θ
ψ = blade azimuth angle

Superscript

$\cdot$ = time derivative
$*$ = equivalent quantity including inflow

Subscripts

I,II = multiblade variable
k = variables for kth blade
$\circ$ = time average

Introduction

PREVIOUS studies of steady state hingeless rotor conditions have shown large reductions in cyclic control hub moments from wake effects.[1-3] In nonsteady rotor conditions the steady state rotor wake, for reasons of numerical stability, has been filtered with arbitrary first order lags.[4] Here a simple nonsteady wake model derived from the unsteady moment of momentum equation for zero advance ratio will be correlated with cyclic pitch frequency response tests conducted with a small hingeless rotor model.[5] The unsteady wake is based on the concept of a participating air mass included in the cylindrical volume of radius R and height h. For an impermeable axially accelerated circular disk the theoretical value of the height of the participating air volume is $h/R = 0.85$, and this value was found to be approximately valid for rotors subject to collective pitch ramp inputs.[6] For our present problem of dynamic cyclic pitch inputs the flow of the participating air volume will be nonuniform and described by a harmonic function of azimuth angle. The height h of the participating air volume will be left open and determined from test results.

Three or More Bladed Rotor Analysis

For a three or more bladed rotor operating at zero advance ratio, assuming straight blades flexibly hinged at the rotor center, the multiblade equations in a nonrotating reference system are[7]

$$\ddot{\beta}_{I} + A\dot{\beta}_{I} + (\omega_1^2 - 1)\beta_{I} + 2\dot{\beta}_{II} + A\beta_{II} = A(\theta_{II} + \lambda_{I}) \quad (1)$$

$$-2\dot{\beta}_{I} - A\beta_{I} + \ddot{\beta}_{II} + A\dot{\beta}_{II} + (\omega_1^2 - 1)\beta_{II} = A(-\theta_{I} + \lambda_{II}) \quad (2)$$

Terms with the factor $A = B^4\gamma/8$ represent aerodynamic hub moments. The multiblade variables with the subscripts I and II are related to the single blade variables used in a rotating frame of reference by

$$\beta_k = \beta_0 + \beta_{I}\cos\psi_k + \beta_{II}\sin\psi_k \quad (3)$$
$$\theta_k = \theta_0 - \theta_{I}\sin\psi_k + \theta_{II}\cos\psi_k \quad (4)$$
$$\lambda_k = \lambda_0 + \lambda_{I}\cos\psi_k + \lambda_{II}\sin\psi_k \quad (5)$$

One finds from the unsteady moment of momentum equations about pitching and rolling axes through the rotor center (See Appendix A)

$$\lambda_{I} + \tau\dot{\lambda}_{I} = -L[\ddot{\beta}_{I} + (\omega_1^2 - 1)\beta_{I} + 2\dot{\beta}_{II}] \quad (6)$$

$$\lambda_{II} + \tau\dot{\lambda}_{II} = -L[\ddot{\beta}_{II} + (\omega_1^2 - 1)\beta_{II} - 2\dot{\beta}_{I}] \quad (7)$$

The inflow gain factor L is proportional to $1/\lambda_0\gamma$, the time constant τ is proportional to Lh/R. The terms in brackets in Eqs. (6) and (7) are equal to the aerodynamic pitching and rolling moments about the rotor center, as can be seen from Eqs. (1) and (2).

Performing the Fourier transforms of Eqs. (6) and (7) and inserting the transformed λ_{I} and λ_{II} into the Fourier transformed Eqs. (1) and (2), one finds that the effect of the dynamic inflow is equivalent to replacing in the equations without inflow the parameter $1/A$ by

$$1/A^* = (1/A) + L/(1 + i\omega_f\tau) \quad (8)$$

or equivalent to replacing the Lock number γ by

$$\gamma^* = \gamma/[1 + B^4\gamma L/8(1 + i\omega_f\tau)] \quad (9)$$

so that Eqs. (1) and (2) become

$$\beta_{I}(-\omega_f^2 + A^*i\omega_f + \omega_1^2 - 1) + \beta_{II}(2i\omega_f + A^*) = A^*\theta_{II} \quad (10)$$

$$\beta_{I}(-2i\omega_f - A^*) + \beta_{II}(-\omega_f^2 + A^*i\omega_f + \omega_1^2 - 1) = -A^*\theta_{I} \quad (11)$$

Received May 29, 1973; revision received September 13, 1973. The work at Washington University was sponsored by AAMRDL, Ames Directorate, under Contract NAS2-4151.
Index category: Rotary Wing Aerodynamics.
*Graduate Research Assistant.
†Professor of Aerospace Engineering, Department of Mechanical and Aerospace Engineering. Associate Fellow, AIAA.
‡Research Scientist, Ames Directorate. Member AIAA.

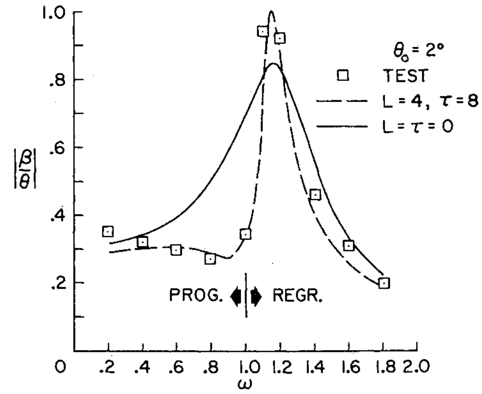

Fig. 1 Amplitude ratio vs frequency, $\theta_0 = 2°$.

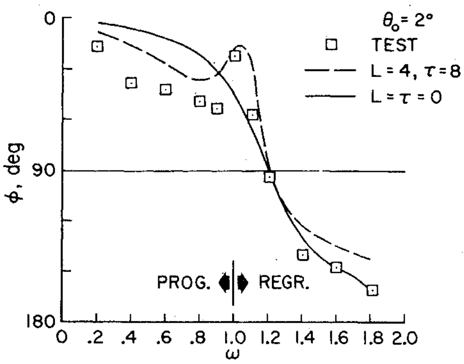

Fig. 2 Phase difference vs frequency, $\theta_0 = 2°$.

Progressing and regressing unit excitation is given respectively by

$$\theta_{\mathrm{I}} = \exp i\omega_f t, \qquad \theta_{\mathrm{II}} = \mp \exp i\omega_f t \tag{12}$$

For a different inflow distribution over the radius the same equations would be obtained with different inflow gain L. Since gain and time constant are to be determined experimentally the actual inflow distribution is properly taken care of.

Two Bladed Rotor Analysis

It can be shown that Eqs. (1) and (2) are equivalent in a rotating frame to the single blade equation[7]

$$\ddot{\beta} + A\dot{\beta} + \omega_1{}^2\beta = A(\theta + \lambda) \tag{13}$$

where at $t = 0$ the blade is located aft. We use the same inflow model defined by the left hand sides of Eqs. (6) and (7) but replace the right hand sides by the proper pitching and rolling moments for a two-bladed rotor

$$\lambda_{\mathrm{I}} + \tau\dot{\lambda}_{\mathrm{I}} = -2L(\ddot{\beta} + \omega_1{}^2\beta)\cos t \tag{14}$$

$$\lambda_{\mathrm{II}} + \tau\dot{\lambda}_{\mathrm{II}} = -2L(\ddot{\beta} + \omega_1{}^2\beta)\sin t \tag{15}$$

Eqs. (14) and (15) can be transformed into a rotating frame of reference by introducing the auxiliary variable§

$$\eta = -\lambda_{\mathrm{II}}\cos t + \lambda_{\mathrm{I}}\sin t \tag{16}$$

By multiplying Eqs. (14) and (15) by cos$t$ and sin$t$ respectively and adding them one obtains with Eq. (5) for $\lambda = \lambda_k - \lambda_0$

$$\tau\dot{\lambda} + \lambda + \tau\eta = -2L(\ddot{\beta} + \omega_1{}^2\beta) \tag{17}$$

By using the factors sin$t$ and $-$cos$t$ and adding

$$\tau\lambda - \tau\dot{\eta} - \eta = 0 \tag{18}$$

The Fourier transforms of Eqs. (13, 17, 18) give

$$\beta/\theta = [(\omega_1{}^2 - \omega^2)\{(1/A) + 2L(1 + \tau^2 + \omega^2\tau^2)/[(1 + \tau^2 - \tau^2\omega^2)^2 + 4\omega^2\tau^2]\} + i\omega\{1 + 2L\tau(\omega_1{}^2 - \omega^2)(\tau^2 - \tau^2\omega^2 - 1)/(1 + \tau^2 - \tau^2\omega^2)^2 + 4\omega^2\tau^2\}]^{-1} \tag{19}$$

§R. A. Ormiston suggested the use of Eqs. (13) to (15) and solved them by the harmonic balance method. S. K. Yin suggested the transformation Eq. (16) and derived Eqs. (17) to (19) with a formally different but numerically identical result.

Comparison with Test Results

For the two bladed rotor model[5] the parameters were $\omega_1 = 1.21$, $A = 0.44$. The inflow gain L and time constant τ were selected by trial and error to obtain a reasonable fit of Eq. (19) to the test results.

Figures 1–4 show amplitude ratio $|\beta/\theta|$ and phase difference $\phi = <\theta - <\beta$ for collective pitch angles of 2° and 8°. The cyclic pitch amplitude was ±1.5°. Each diagram represents test results and analytical results with and without dynamic wake. The measured amplitude ratios agree quite well with the analytical ratios, using $L = 4$, $\tau = 8$ for 2° collective pitch, and $L = 2$, $\tau = 4$ for 8° collective pitch. The phase angles show less agreement, particularly at 8° collective pitch. A possible explanation for the latter case is the angular deflection of the steady wake which may produce an inplane wake component not considered in the analysis. The tests were conducted with a ground plate varying in distance from the rotor center between $0.5R$ and $1.5R$ and without ground plate. No substantial differences in test results were found.

Four bladed hingeless rotor models with the capability of exciting progressing and regressing flapping motions will be tested both at AAMRDL (7.5 ft D) and at Washington University (1.5 ft D) and may shed some further light on the problems of unsteady wake effects.

Appendix A: Derivation of Eq. (7)

We assume that the flow through the rotor disk consists of a uniform constant velocity v_0 positive up and a harmonic time variable velocity $v \sin\psi$. In the fully developed

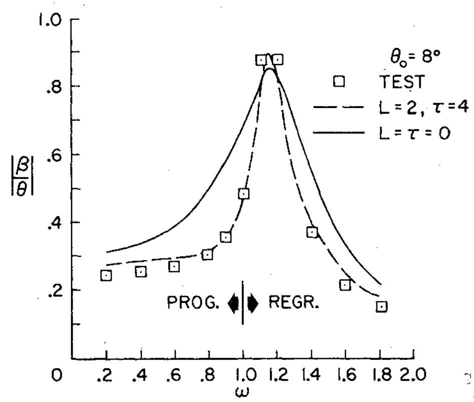

Fig. 3 Amplitude ratio vs frequency, $\theta_0 = 8°$.

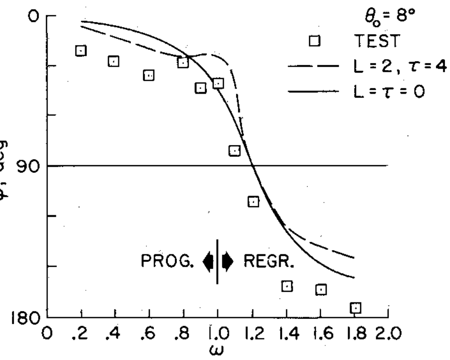

Fig. 4 Phase difference vs frequency, $\theta_0 = 8°$.

wake the velocities are $2(v_0 + v \sin\psi)$. The air, participating in the acceleration $\dot{v} \sin\psi$ is assumed to be enclosed in a cylinder with radius R and height h. The moment of momentum equation about the longitudinal axis contains only terms with factor $\sin^2\psi$ and reads

$$-\int_0^{2\pi}\int_0^R r d\psi dr \cdot r \sin\psi \rho(4v_0 v \sin\psi + h\dot{v} \sin\psi) = C_l(\Omega R)^2 \rho\pi R^2 \quad \text{(A1)}$$

where C_l is the aerodynamic hub rolling moment coefficient, positive to right. Performing the integrations and using nondimensional velocities $\lambda_0 = v_0/\Omega R$, $\lambda_{II} = v/\Omega R$ and the time unit $1/\Omega$, one obtains

$$\lambda_{II} + \tau\dot{\lambda}_{II} = -3C_l/4\lambda_0 \quad \text{(A2)}$$

where

$$\tau = h/4\lambda_0 R \quad \text{(A3)}$$

Performing the same analysis with a radially linear inflow velocity distribution assumed in Eqs. (1) and (2), one obtains

$$\lambda_{II} + \tau\dot{\lambda}_{II} = -5C_l/16\lambda_0 \quad \text{(A4)}$$

where

$$\tau = 5h/16\lambda_0 R \quad \text{(A5)}$$

In either case the expression $\lambda_{II} + \tau\dot{\lambda}_{II}$ is proportional to the left aerodynamic hub rolling moment, which is expressed in Eq. (7). Since τ and L are determined by correlation with tests, Eqs. (6) and (7) do not assume any specific inflow distribution over the radius.

References

[1]Miller, R. H., "Rotor Blade Harmonic Airloadings," *AIAA Journal*, Vol. 2, No. 7, July 1964, p. 1260.

[2]Curtiss, H. C. Jr., "The Use of Complex Coordinates in the study of Rotor Dynamics," *Journal of Aircraft*, Vol. 10, No. 5, May 1973, pp. 285–295.

[3]Ormiston, R. A. and Peters, D. A., "Hingeless Rotor Response with Non-Uniform Inflow and Elastic Blade Bending," *Journal of Aircraft*, Vol. 9, No. 10, Oct. 1972, pp. 730–736.

[4]Kerr, A. W., Potthast, A. J., and Anderson, W. D., "An Interdisciplinary Approach to Integrated Rotor/Body Mathematical Modeling," *Mideast Region Symposium*, American Helicopter Society, 1972.

[5]Hohenemser, K. H. and Crews, S. T., "Model Tests on Unsteady Rotor Wake Effects," *Journal of Aircraft*, Vol. 10, No. 1, Jan. 1973, pp. 58–60.

[6]Carpenter, P. J. and Fridovich, B., "Effect of a Rapid Blade Pitch Increase on the Thrust and Induced Velocity Response of a Full Scale Helicopter Rotor," TN 3044, Nov. 1953, NACA.

[7]Hohenemser, K. H. and Yin, S. K., "Some Applications of the Method of Multiblade Coordinates," *Journal American Helicopter Society*, Vol. 17, No. 4, July 1972, pp. 3–12.

Dynamics of Slung Bodies Utilizing a Rotating Wheel for Stability

Edward C. Micale* and Corrado Poli†
University of Massachusetts, Amherst, Mass.

Nomenclature

a,h	= horizontal and vertical distances between attachment points
d_1,d_2	= horizontal and vertical distances from the center of mass of the box to the cable attachment point along x, y, z
A,B,C	= moments of inertia of rectangular cargo container about the x, y, z axes
A_1,C_1,A_1	= moments of inertia of wheel about x_1, y_1, z_1 axes
D/W	= drag-to-weight ratio
l	= cable length
L,M,N	= aerodynamic moments
m_T	= mass of towed system
m_1	= mass of wheel
r	= wheel radius
R_1	= vertical distance from c.m. box to c.m. wheel along z
T_0	= steady-state cable force
u,v,w	= linear perturbation velocities
U_0	= x component of steady state velocity
W_0	= z component of steady state velocity
W_1/W	= wheel weight to system weight ratio
ω_1	= wheel rotational speed
X,Y,Z	= aerodynamic forces
θ,ψ,ϕ	= aircraft Euler angles
α	= angle of attack
α_0	= steady state angle of attack
β	= side-slip angle
C_D	= drag coefficient
C_L	= lift coefficient
C_Y	= side-force coefficient
C_l	= roll moment coefficient
C_m	= pitch moment coefficient
C_n	= yaw moment coefficient
C_{L_α}	= $\partial C_L/\partial\alpha$
C_{m_α}	= $\partial C_m/\partial\alpha$
C_{Y_β}	= $\partial C_y/\partial\beta$
C_{n_β}	= $\partial C_n/\partial\beta$
X_u,X_w, etc.	= changes in the aerodynamic forces and moments due to changes in velocities

Introduction

IN the past few years airborne towing has proven to be very useful for industrial and military transportation. Even though this means of transportation has demonstrated its effectiveness, reports have revealed that quite often serious instabilities have occurred. Asseo and Erickson[1] mention the dangerous load oscillations experienced while towing low density, high drag loads, which have resulted in emergency load jettison and some load/helicopter collisions. Similarly Etkin and Mackworth[2] report of serious instabilities which occurred while transporting loads of dense material in a specially designed bucket. Experimental investigations by Shanks[3-5] showed that lateral instability may arise in towing parawing gliders and half-cone re-entry vehicles. These problems have resulted in a number of investigations to determine the criteria necessary to insure stability during airborne towing.

Received June 18, 1973. This work was supported by the U.S. Army Research Office—Durham.

Index categories: Air Transportation Systems; VTOL Handling, Stability, and Control.

*Graduate student, Mechanical and Aerospace Engineering Department.

†Professor, Mechanical and Aerospace Engineering Department.